MSME Laboratoire Modélisation et Simulation Multi Echelle

CARACTÉRISATION STATISTIQUE DE LA MICROSTRUCTURE ET PROPRIÉTÉS EFFECTIVES DE MATÉRIAUX ACOUSTIQUES

By Camille Perrot

MSME, Univ Gustave Eiffel, UPEC, CNRS, F-77454 Marne-la-Vallée, France

Email: camille.perrot@univ-eiffel.fr

- **General objective.** Estimate the macroscopic properties of acoustic materials from easily measurable geometrical quantities
- **Approach**. Situated between different disciplines.
- Imaging techniques provide most of the data
- Stochastic geometry plays a role in the reconstruction of porous media
- Homogenization develops the main tools of analysis such as flow and permeability calculations
- Laboratory experiments (validation)

Stochastic Microstructures and Properties

- **Description and terminology**. It may be convenient to start with real examples which can be seen almost everywhere.

Fig. 1.2.1 A view of a fibrous material

(a) sample or panel ~ m,

(b) mesoscopic fluctuations ~ cm,

(c) a porous medium ~ µm (solid phase and fluid phase).

- Porosity
- Monodisperse, polydisperse (same/different size)
- Pores size << wavelength

○ **Objectives and organization of this talk**.

- **Objective**. Determination of the intrinsic macroscopic properties of two acoustic materials (fibrous networks, cellular foams) from easily measurable geometric quantities.
- **Methodology**.

1. First, since geometry plays such a crucial role, the various structures are quantitatively described
2. Second, the intrinsic macroscopic properties of each structure are determined.

   This requires going from one scale to the next larger one; the local equations on the small scale are solved and the solutions are averaged on the larger scale.
3. The numerical results needs to be rationalized (parametric analysis, physical trends, guiding manufacturing process).

⟶ This methodology is the read thread which marks the parts of this talk.

- **Structure of this talk.**

2.1 Generation of fibrous media (acquisition)

Distribution of: (i) fiber diameters, (ii) fiber lengths, (iii) angular orientation of fibers (horizontal and vertical). Presence of a binder [PhD Thesis Mu HE, U. Paris-Est].

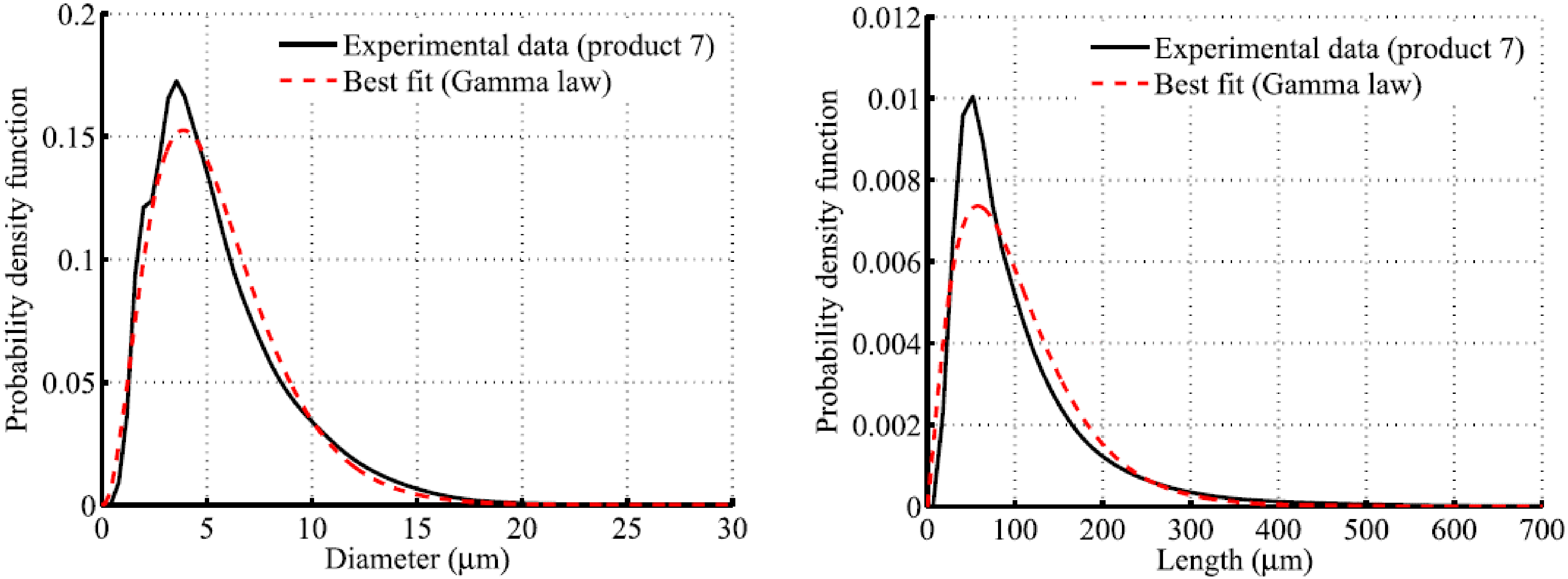

Fig. 2.1.1 Estimated probability density functions of (a) fiber diameters (left) and fiber lengths (right) [J. Acoust. Soc. Am. 143, 3283 (2018)].

2.1 Generation of fibrous media (acquisition)

Distribution of: (i) fiber diameters, (ii) fiber lengths, (iii) angular orientation of fibers (horizontal and vertical). Presence of a binder.

[PhD Thesis, M. HE, U. Paris-Est (2018)].

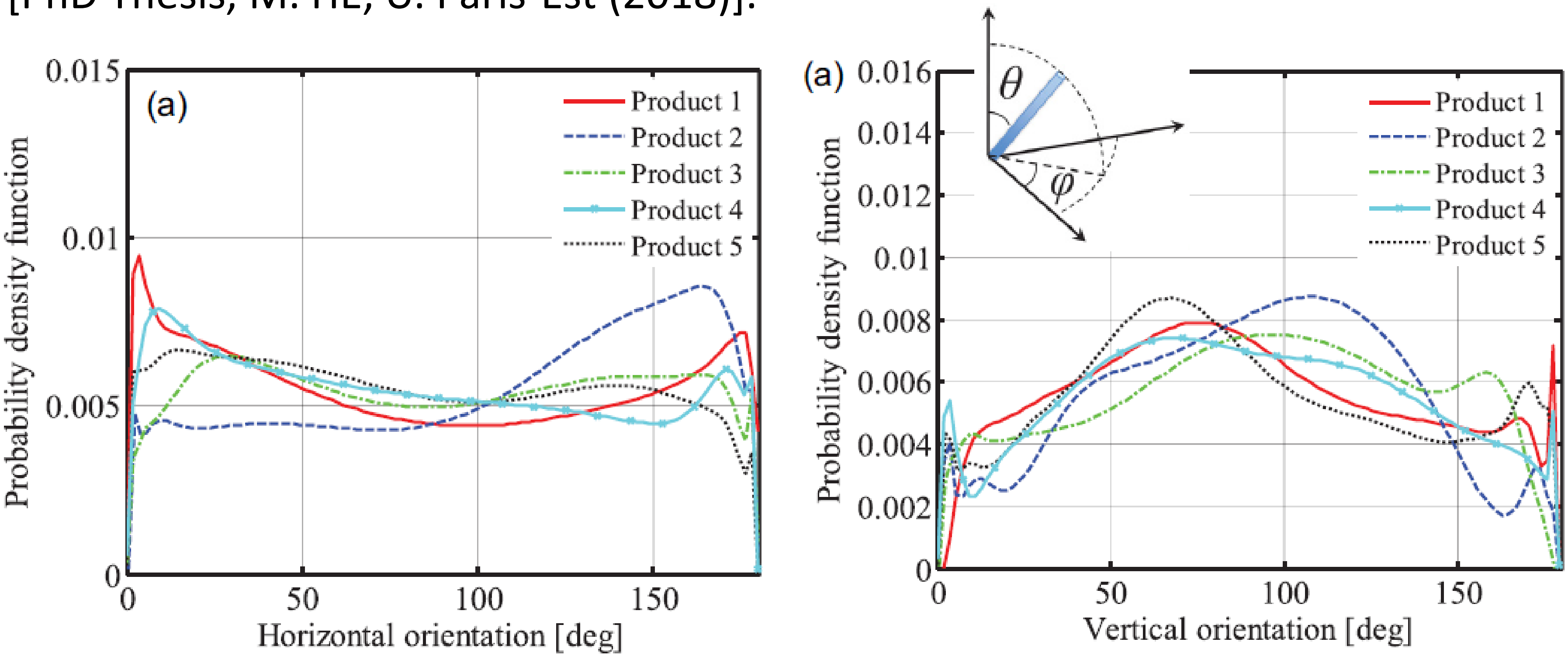

Fig. 2.1.2 Estimated probability density functions of horizontal orientation angle φ (left), and vertical orientation angle θ (right) [J. Acoust. Soc. Am. 143, 3283 (2018)].

2.1 Generation of fibrous media (deterministic models)

- Parallel solid cylinders. Longitudinal or transverse directions (Tarnow et al., Umnova et al., Boutin, Piegay et al.).
- A three-dimensional deterministic model with a fiber connectivity of eight

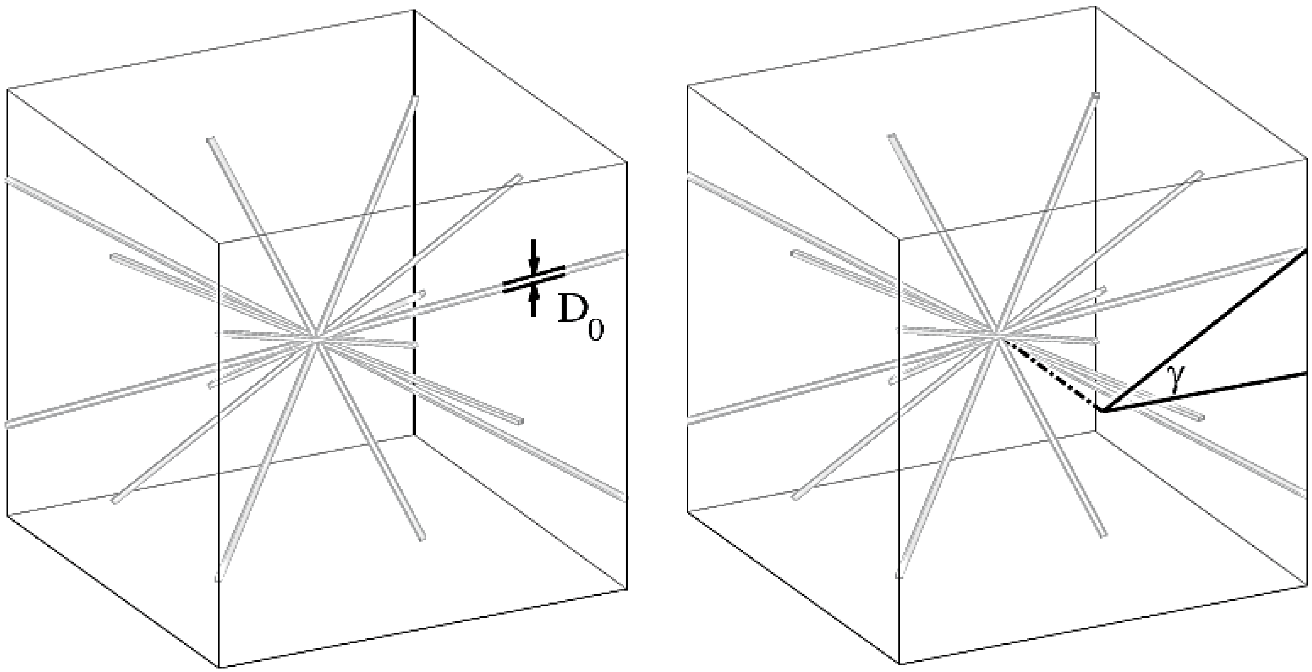

Fig. 2.1.3 Illustration of the proposed equivalent microstructure, parameterized by a mean (averaged) diameter D_0 and mean angular orientation $\gamma = \theta - \frac{\pi}{2}$ derived from distributions [J. Acoust. Soc. Am. 143, 3283 (2018)].

2.1 Generation of random fibrous media (reconstruction)

- The concept of tensor of angular orientation
- In this example, the random fiber structures result from the successive generation of rigid uniform cylinders of the same diameter.
- Let 's associate a vector **p** to the fiber.

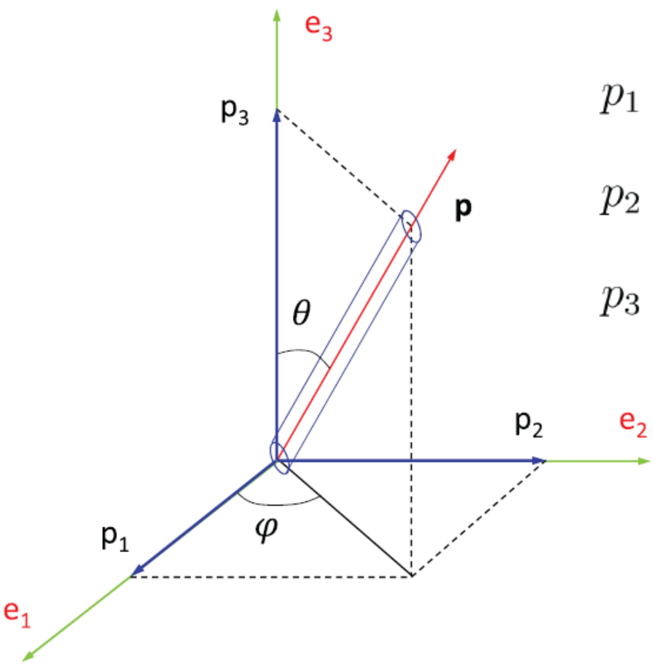

$$p_1 = sin\theta cos\varphi$$

$$p_2 = sin\theta sin\varphi$$

$$p_3 = cos\theta$$

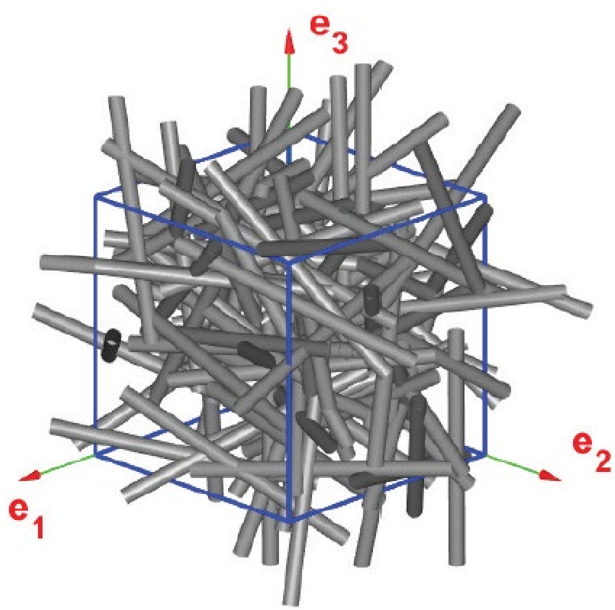

- Random structure defined as an arrangement of fibers for which the orientation distribution ψ(φ, θ) is a function of two variables defining the orientation of a fiber.

2.1 Generation of random fibrous media (reconstruction)

- The use of tensor to describe fiber orientation of composite fibers
  [Advani and Tucker, J. Rheol. 31, 751 (1987)]
- The second order orientation tensor Ω_{ij} is obtained by forming diadic products of the vector **p** and then averaging the products with the distribution function ψ over all possible directions:

$$\Omega_{ij} = \int p_i p_j \Psi(\overrightarrow{p}) d\overrightarrow{p}$$

- For a discrete set of fibers:

$$p_1 = sin\theta cos\varphi$$
$$p_2 = sin\theta sin\varphi$$
$$p_3 = cos\theta$$

$$[\Omega] = \frac{1}{N_f}\sum_{i=1}^{N_f}\begin{bmatrix} sin^2\theta^{(i)}cos^2\varphi^{(i)} & sin^2\theta^{(i)}cos\varphi^{(i)}sin\varphi^{(i)} & sin\theta^{(i)}cos\theta^{(i)}cos\varphi^{(i)} \\ sin^2\theta^{(i)}cos\varphi^{(i)}sin\varphi^{(i)} & sin^2\theta^{(i)}sin^2\varphi^{(i)} & sin\theta^{(i)}cos\theta^{(i)}sin\varphi^{(i)} \\ sin\theta^{(i)}cos\theta^{(i)}cos\varphi^{(i)} & sin\theta^{(i)}cos\theta^{(i)}sin\varphi^{(i)} & cos^2\theta^{(i)} \end{bmatrix}$$

- Properties: [Ω] is symmetric. Since Trace [Ω] = 1 (renormalization condition), for transversely isotropic materials [Ω] completely determined by Ω_{zz} .

2.1 Generation of random fibrous media (reconstruction)

- By varying Ω_{zz} from planar ($\Omega_{zz} = 0$) to aligned ($\Omega_{zz} = 1$) random fibers, one can study the influence of fiber orientation on the transport properties of random fibrous media.

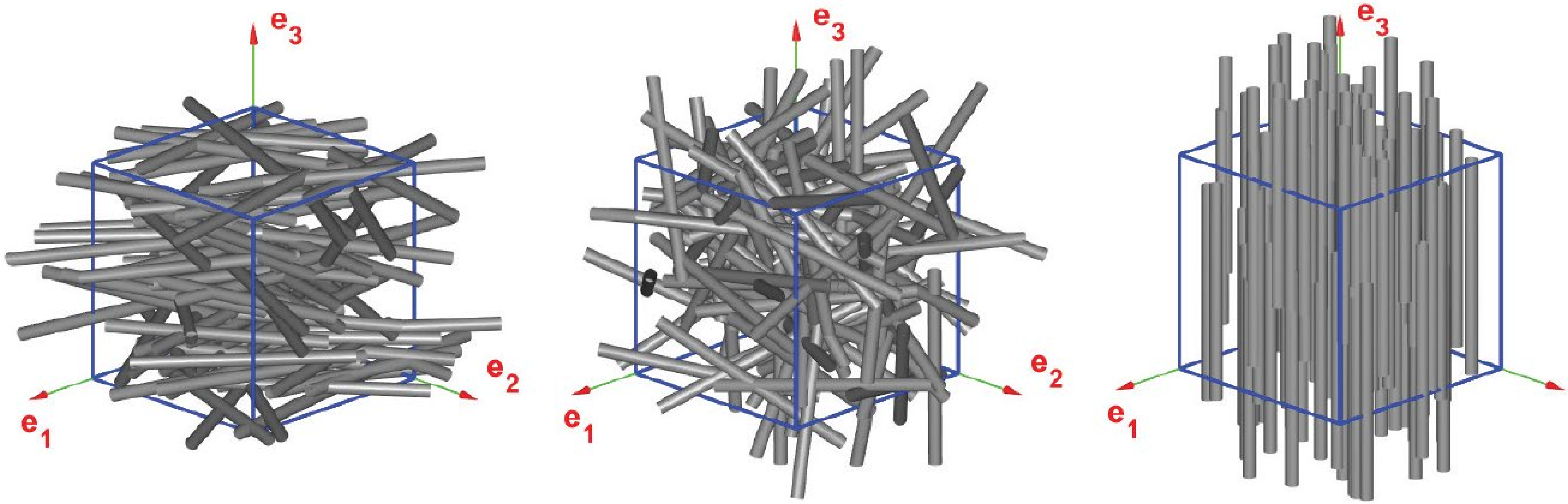

Fig. 2.1.4 Systematic generation of random fibrous media [Acta Acust. Unied Ac. 103, 1050 (2017)]

- Done by adjusting (μ_θ, σ_θ) of a normal distribution for θ; with a uniform distribution for φ [PhD Thesis H. T. Luu, U. Paris-Est and U. Sherbrooke (2016)].

2.2 Generation of cellular foams (acquisition)

- Distribution of cell size
- Distribution of cell elongation
- The presence of membranes (proportion and opening ratio)

PhD Thesis, C. T. Nguyen, U. Gustave Eiffel, 2021

See also [Int. J. Solid. Structures 249, 111684 (2022)]

Tomographic Reconstruction and Morphological Analysis

Detection and pore size distribution from X-ray µCT and image analysis

A. Original image of microtomography.
B. Binarized image generating the struts system of foam
C. Image obtained after distance transform (maxima, cell centers) and inversion
D. Detected pores after segmentation by watershed transform
E. 3D visualization of struts system
F. and the corresponding detected pores.

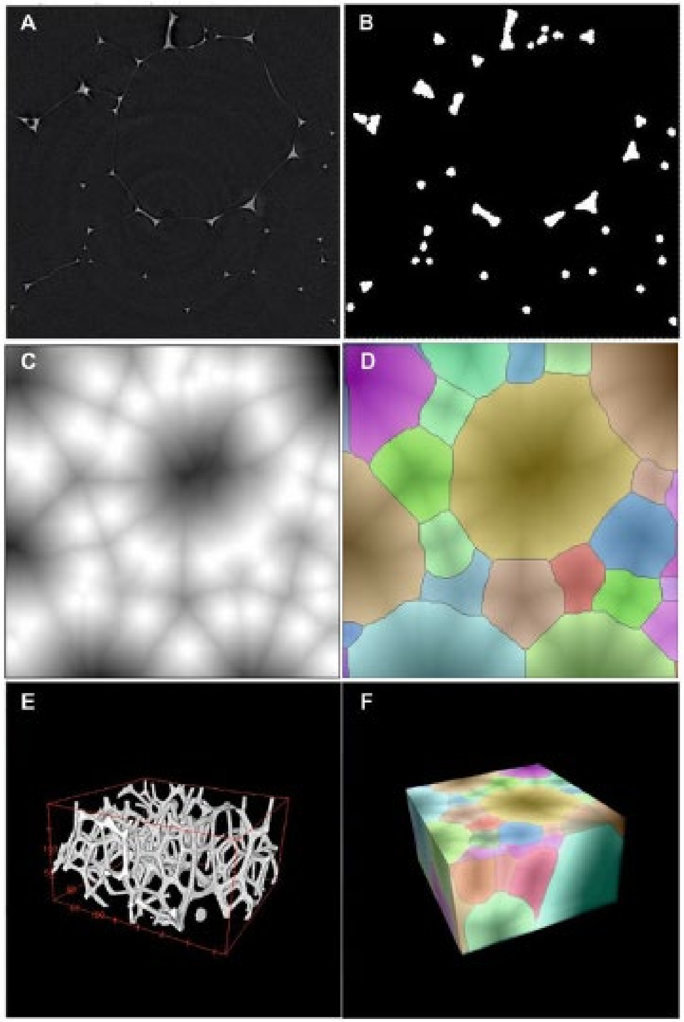

6 x 6 x 6 mm^3 ; 2131 pores; 6 µm

o **Procedure** described in [A. Nistor et al, "Tomographic reconstruction and morphological analysis of rigid polyurethane foams," Macromol. Symp. 360, 87–95 (2016)]

o Image **processing steps** carried out using the **open-source** FIJI software with the plugins MorphoLibJ.

Pore Size Distribution and the Sphericity Index

- Pore size represented by an equivalent diameter *d*, the diameter of a sphere with a volume equivalent to the volume of the corresponding pore.
- Sphericity index *s*, defined as the ratio of the surface area of the sphere of equivalent volume over the surface area of the corresponding pore (1 for a sphere, smaller values otherwise).

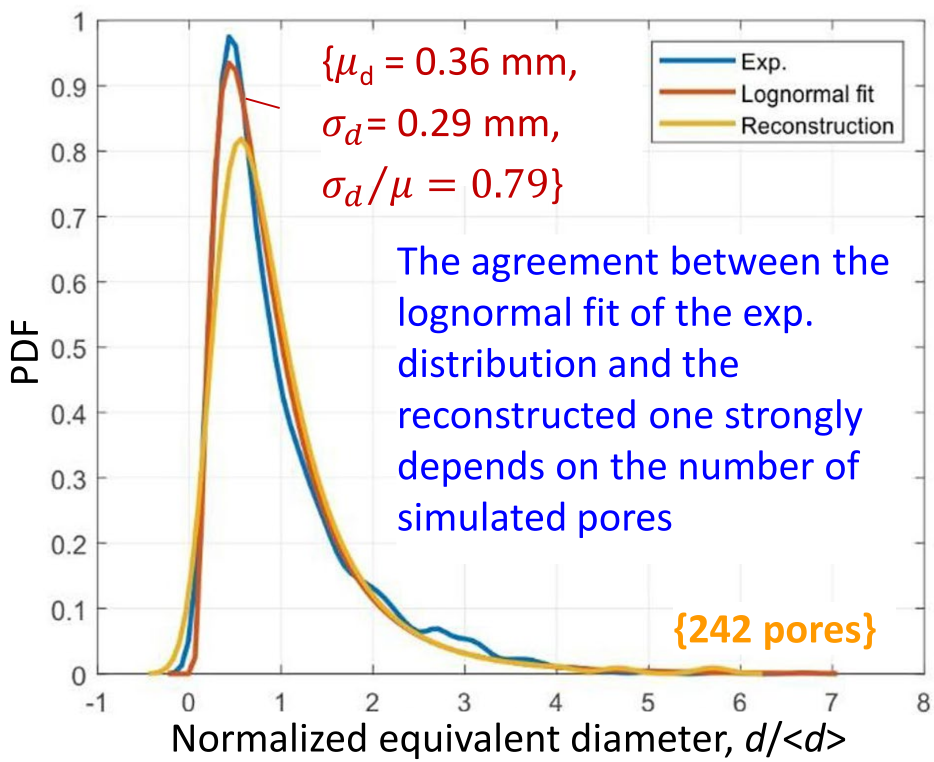

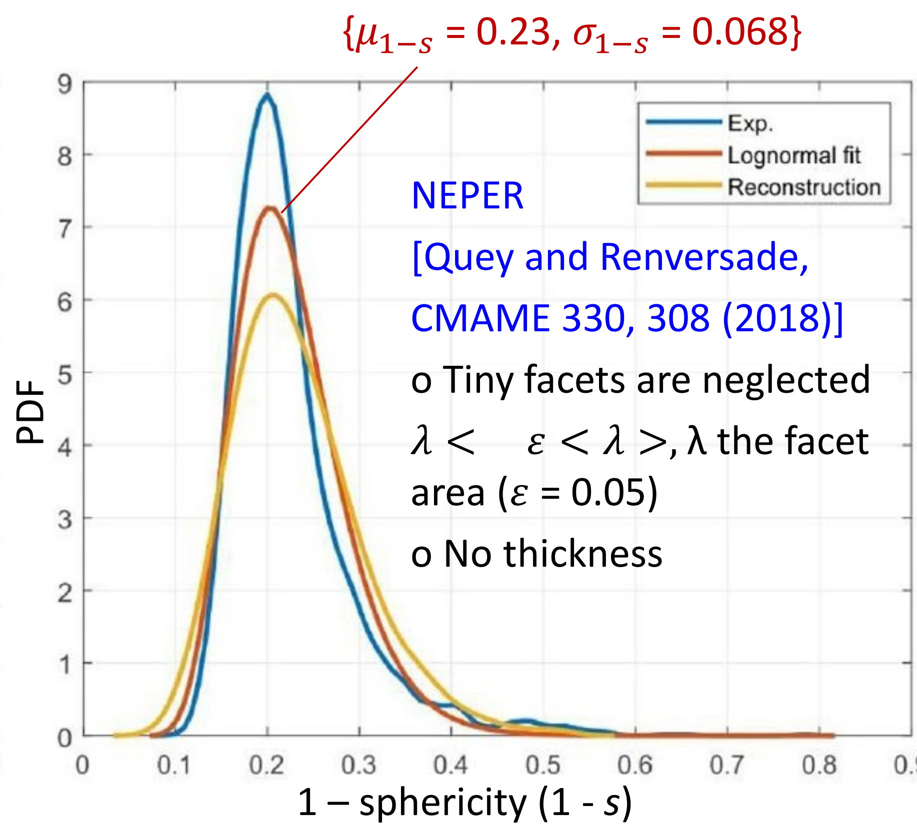

Membrane Characteristics

- The characterization of membranes is performed by analyzing the surfaces of the foam sample through scanning electron microscope (SEM) images.
- Both the
  - i) proportion of closed membranes x_c;
  - ii) aperture ratio of open membranes $t_0 = \sqrt{A_{el}/A_{pl}}$;

  are taken into account in the model.

  The average of aperture ratio $\langle t_0 \rangle$ is also deduced.

o $\langle x_c \rangle = 0.76$; $\langle t_0 \rangle = 0.17$

o Membrane thickness ~ 1 - 2 µm << $\langle d \rangle = 360$ µm

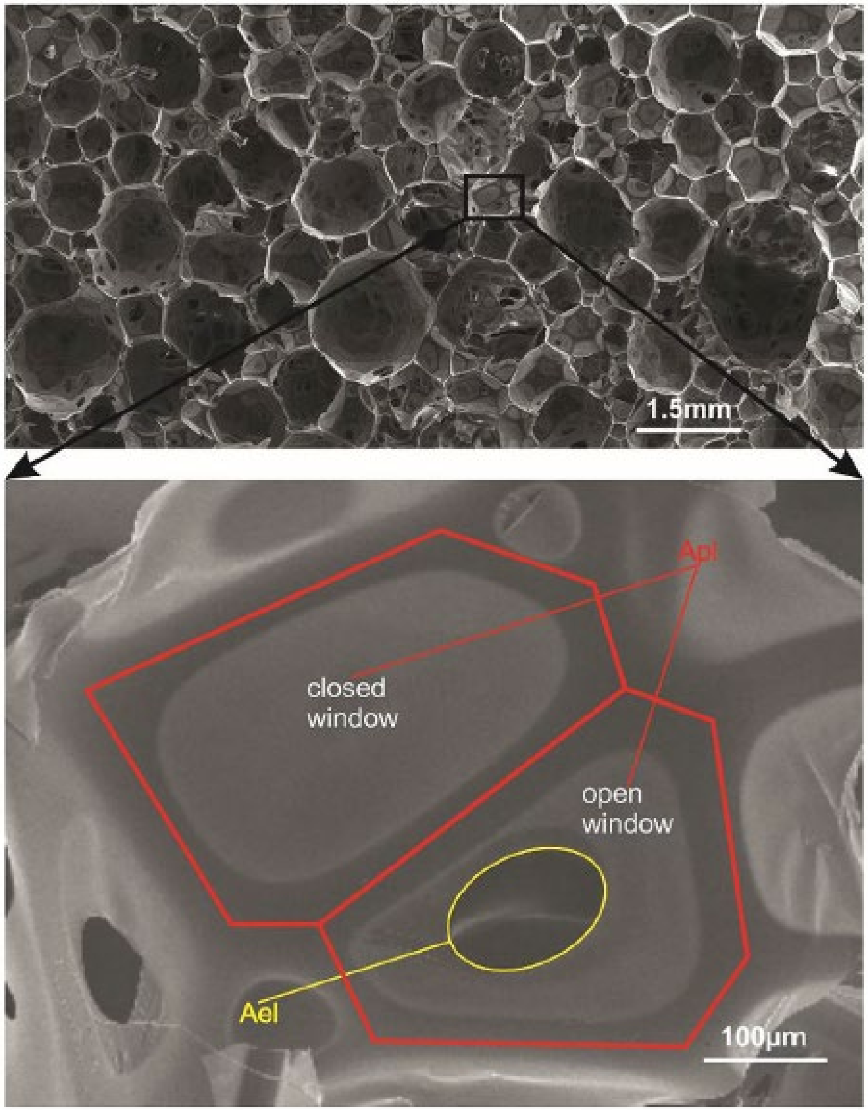

Generation of random cellular media (reconstruction)

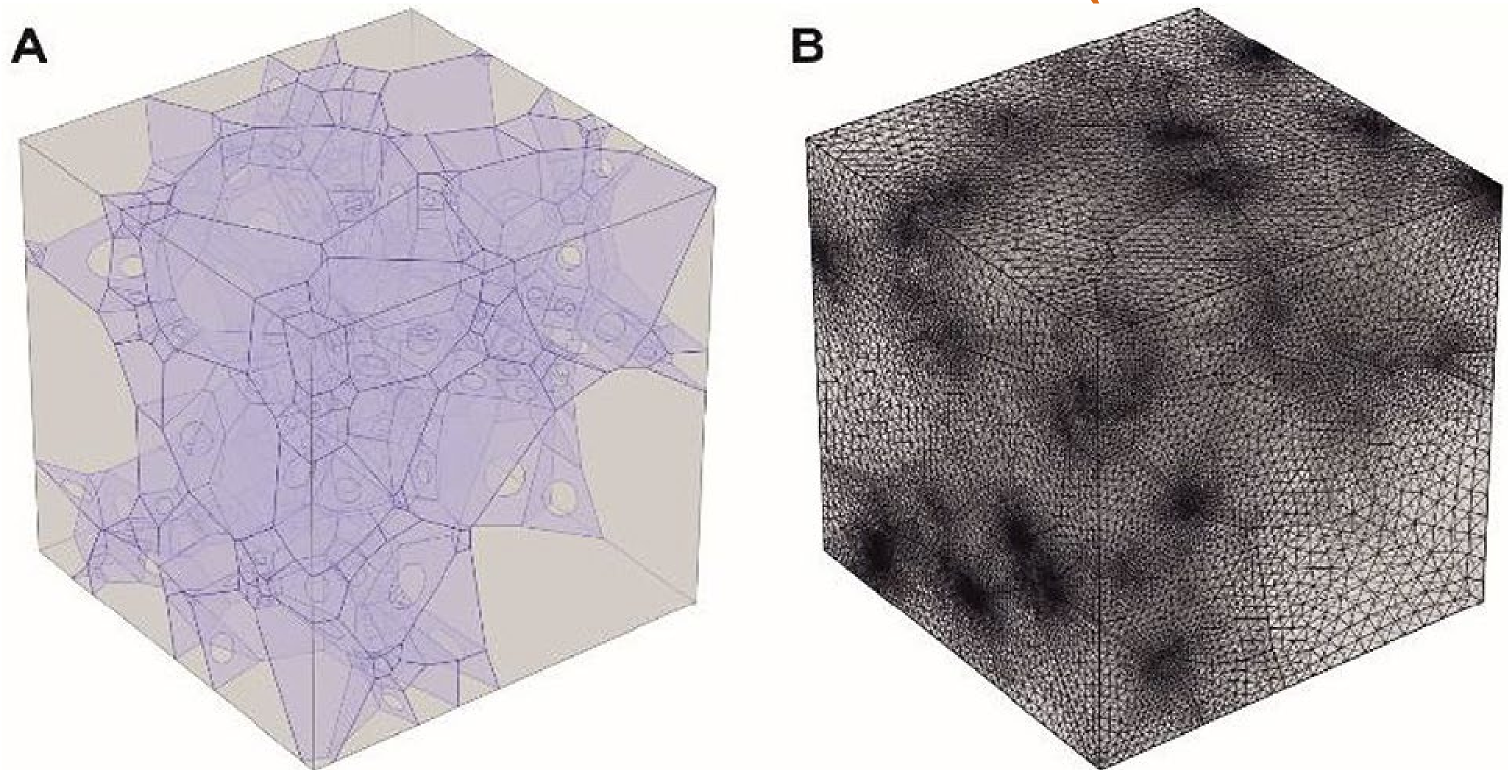

- Generated geometry with $\sim 8^3$ cells (A) and corresponding mesh (B) with 7 360 100 tetrahedral elements
- The open membranes are randomly selected among all the membranes
- Among the opened membranes, the membranes are locally opened with an aperture ratio equal to $\langle t_0 \rangle$

3.1 Elementary transport and elastic properties

- This section details the analysis of **elementary transport** (viscous fluid flow, electric conductivity, diffusion of heat).
- The main objective of this sec. is to recall **how macro intrinsic properties of porous media can be derived** from elementary boundary value problems when their geometrical characteristics are known (this approach may be extended to other phenomena).
- This is important because these intrinsic macroscopic properties have a **clear definition with a physical meaning**, their calculations can therefore be compared with experimental values and quantitatively discussed.
- Semi-phenomenological models or frequency-dependent calculations provide the missing **link** with the dynamic macroscopic behavior (sound absorption, transmission loss); see [Johnson et al, 1987; Lafarge et al, 1997; Biot, 1956 ab] {Biot-JCAL model}.
- Under **scale separation**, mathematical **foundations** can be justified from the Homogenization of Periodic Media (HPM); see [Auriault, Boutin, Geindreau, Homogenization of Coupled Phenomena in Heterogeneous Media, 2009].

3.2 Flow of a Newtonian fluid

3.2.1) Rigorous approach

Stokes equations

$$\eta\nabla^2\vec{v} - \vec{\nabla}p = -\vec{G}$$

$$\vec{\nabla}\cdot\vec{v} = 0$$

$$\vec{v} = 0 \quad on \quad \partial\Omega$$

$\vec{v}$ and p spatially periodic

$\vec{v}$ velocity
p pressure
η dynamic viscosity
$\vec{G} = \vec{\nabla}p^m$
macroscopic pressure gradient

3.2.2) Estimation of the viscous permeability

→ Effective pore surface area for viscous flow

- Permeability tensor : $k_{0ij} = \phi\left\langle k^*_{0ij}\right\rangle$

  defined from

  $$v_i = -\frac{k^*_{0ij}}{\eta}G_j$$

- Kozeny-Carman equation: $\frac{k_0}{r_f^2} = \zeta\frac{\phi^3}{(1-\phi)^2}$

ζ is the Kozeny "constant"

3.2.3) Analytical or semi-analytical solutions

- Flow past cylinders or spheres (Tarnow, 1996; Umnova et al, 2000)
- Self consistent models (Boutin, 2000; Boutin and Geindreau, 2008 and 2010; Piegay et al, 2020)
- Sampson law and pore network calculations (Langlois et al, 2018)

3.3 Flow of an inviscid fluid

3.3.1) Rigorous approach

Electric conduction problem (potential flow)

$$\vec{E} = -\vec{\nabla}\pi + \vec{e}$$

$$\vec{\nabla} \cdot \vec{E} = 0$$

$$\vec{E} \cdot \vec{n} = 0 \quad \text{at the wall } \partial\Omega$$

π $\vec{E}$ spatially periodic

where

- $\vec{E}$ electric field
- π microscopic potential
- $\vec{e}$ macroscopic electric field.
- $\vec{n}$ unit normal vector to $\partial\Omega$

3.3.2) Estimations of the tortuosity and viscous length

- Tortuosity tensor : $e_i = \alpha_{\infty ij} \langle E_j \rangle$

⟶ Microscopic velocity dispersion $\alpha_\infty = \phi \dfrac{\langle \boldsymbol{E} \rangle^2}{\langle \boldsymbol{E} \rangle^2}$

- Viscous characteristic length Λ :

⟶ Throat radius $$\Lambda = 2\frac{\int_\Omega ||\vec{E}||^2 dV}{\int_{\partial\Omega} ||\vec{E}||^2 dS}$$

3.3.3) Analytical or semi-analytical solutions

- Flow past cylinders or spheres (Champoux and Allard, 1998; Umnova et al, 2000)
- Self consistent models (Boutin and Geindreau, 2008 and 2010; Piegay et al, 2020)
- Sampson law and pore network calculations (Langlois et al, 2019)

3.4 Diffusion of heat

3.3.1) Rigorous approach

Diffusion controlled reactions

$$\nabla^2 \tau = -1$$

$$\tau = 0 \quad \text{on} \quad \partial\Omega$$

τ is spatially periodic.

τ excess temperature

3.3.2) Estimations of the thermal permeability

- Static thermal permeability $k'_0 = \phi \langle \tau \rangle$

  $\longrightarrow$ Effective pore surface area for heat diffusion

- Thermal characteristic length $\Lambda' = \dfrac{2V_p}{S_w}$

  $\longrightarrow$ Generalized hydraulic radius

3.3.3) Analytical or semi-analytical solutions

- Flow past spheres (Umnova et al, 2000)
- Self consistent models (Boutin and Geindreau, 2010; Piegay et al, 2020)

4.1 Results for fibrous media and discussion

Correlation proposed to approximate properties when geometry is known

Example: Static viscous permeability

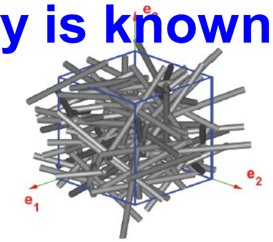

Simulations fit with $$log_{10}\left(\frac{k_0}{r_f^2}\right) = Alog_{10}\left(\frac{\phi^3}{(1-\phi)^2}\right) + B\Omega_{zz}^2 + C\Omega_{zz} + D$$

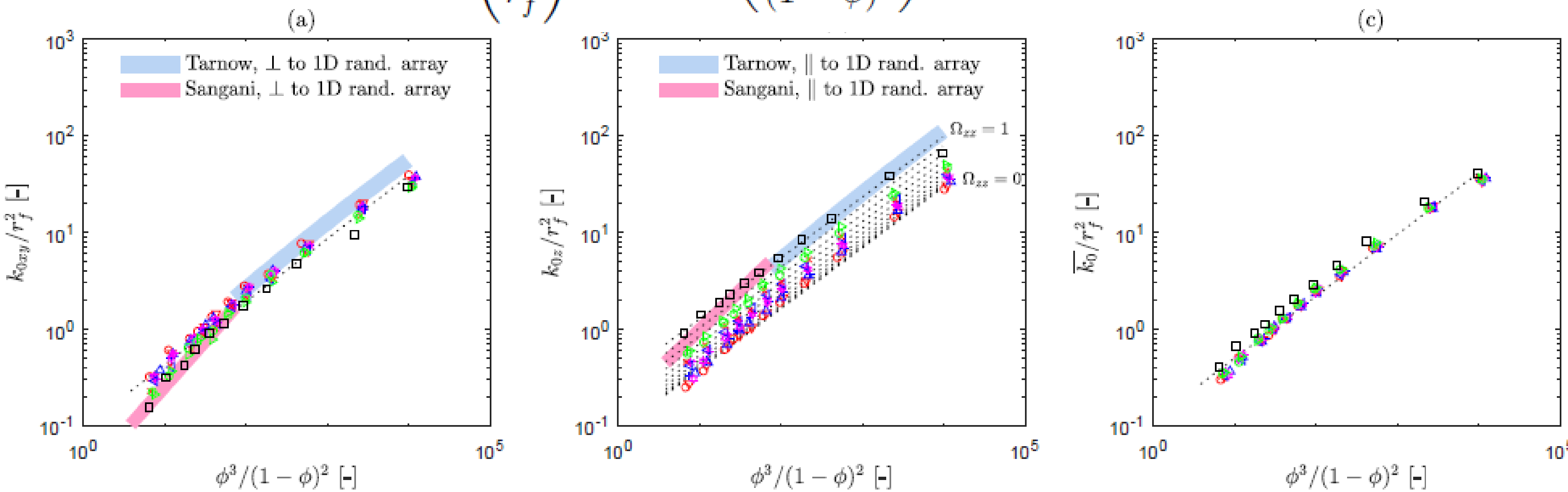

✓ The through plane permeability k_{0z} is more sensitive to fiber orientation Ω_{zz} than the in-plane permeability k_{0xz}:

(a) k_{0xy} varies linearly with $\phi^3/(1-\phi)^2$, which is consistent with the KC Eq.

(b) k_{0z} also depends on Ω_{zz}.

4.1 Results for fibrous media and discussion

Geometrical models: Deterministic and fully stochastic

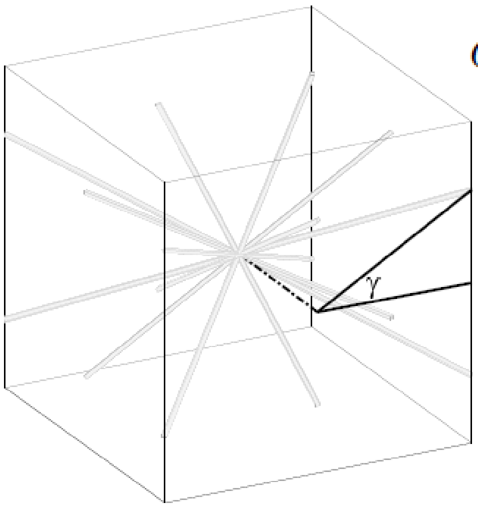

$$\phi_0(D_w/L, \gamma^{exp}) = \phi_0(D_0/L_0, \gamma^{exp}) = \phi^{exp}$$

$$D_w = \frac{1}{\sum_{i=1}^{N_f} V_i} \sum_{i=1}^{N_f} V_i D_i$$

Model 1

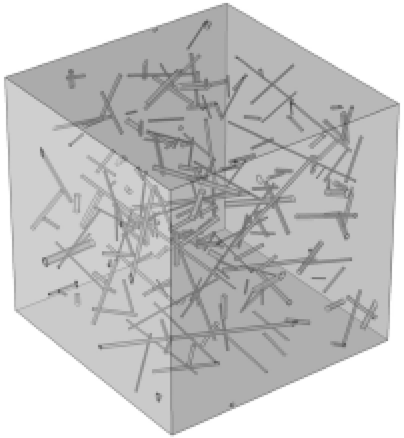

No weighting

Model 2

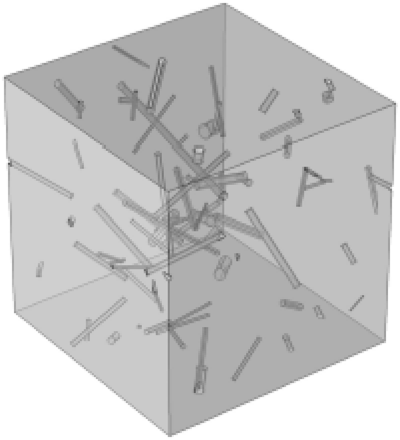

Volume weighting averaging

Model 3

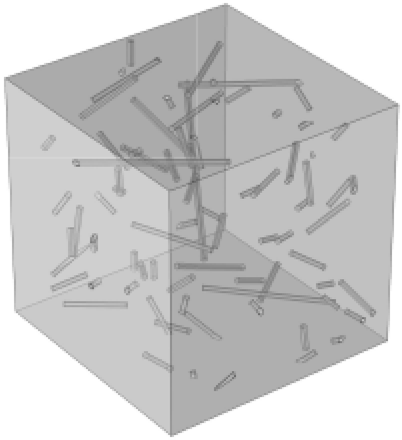

Volume weighting averaging – Mean

4.1 Results for fibrous media and discussion

Comparison with experimental results

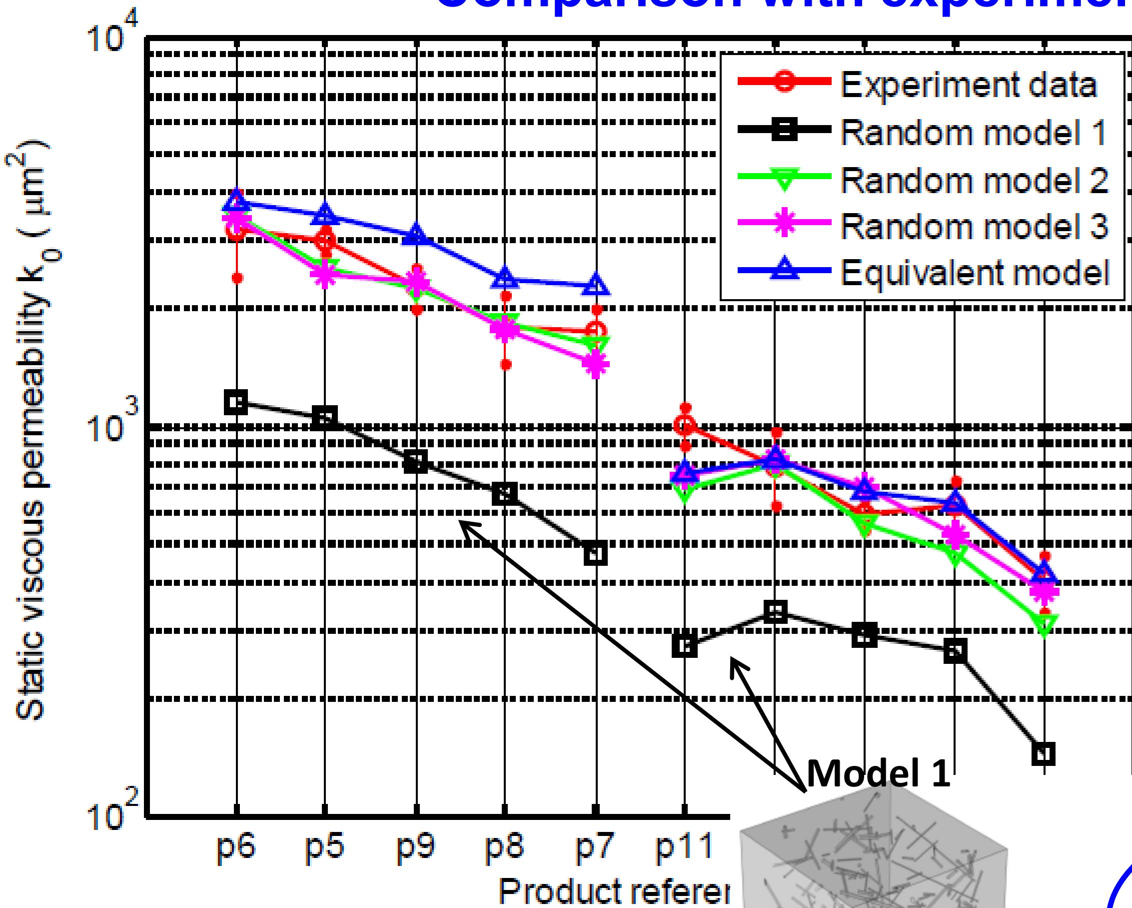

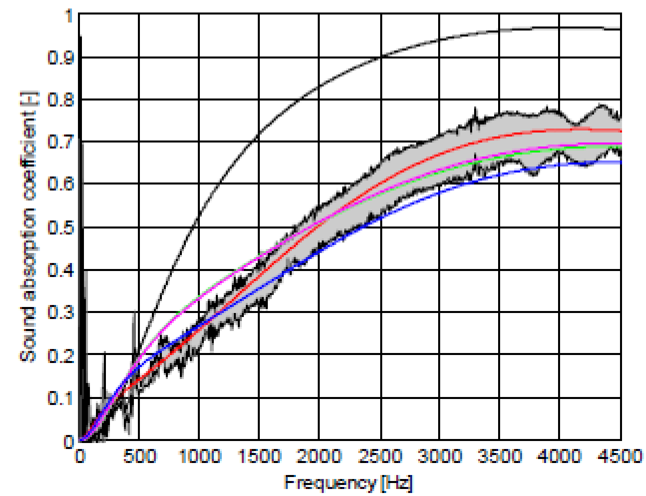

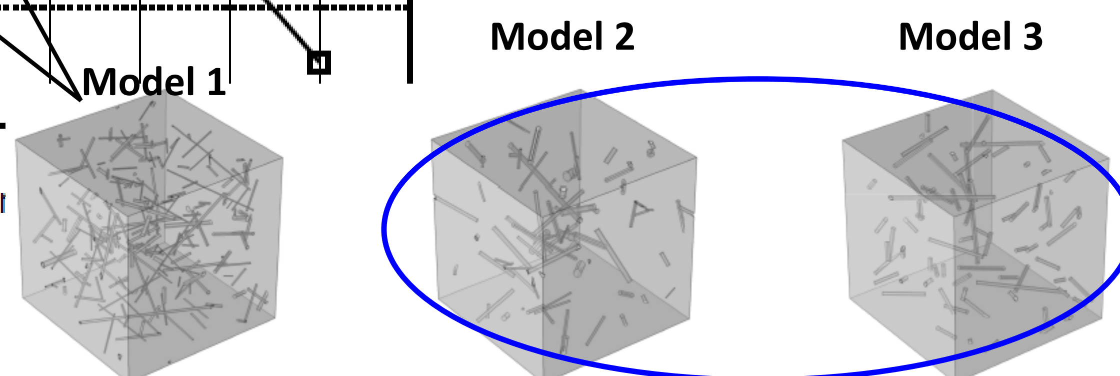

[J. Acoust. Soc. Am. 143, 3283 (2018)]

4.1 Results for fibrous media and discussion

Comparison with experimental results

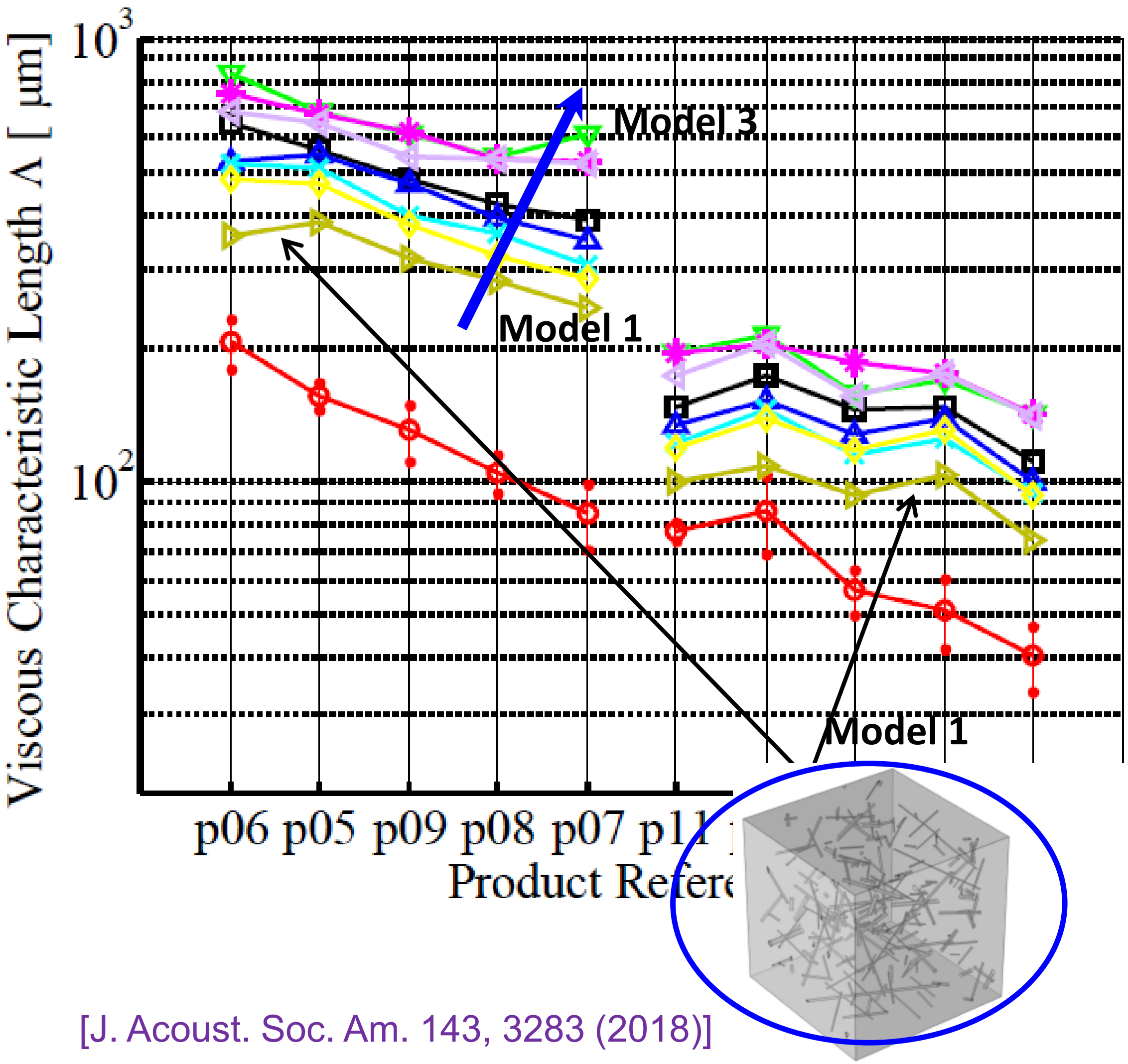

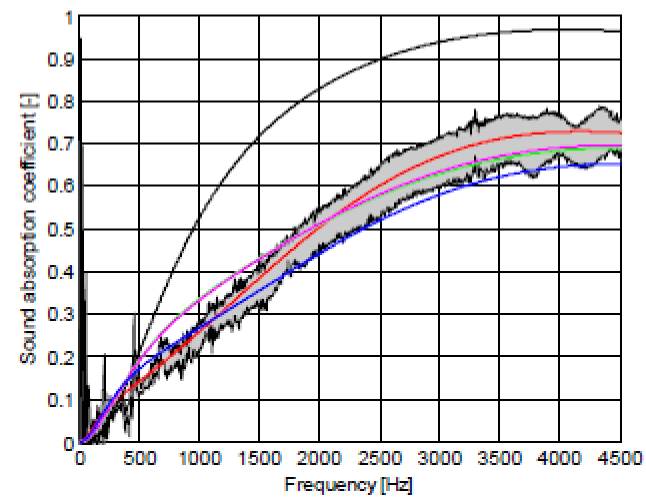

Model 2

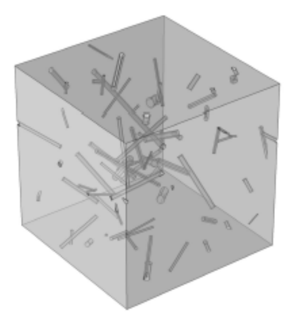

Model 3

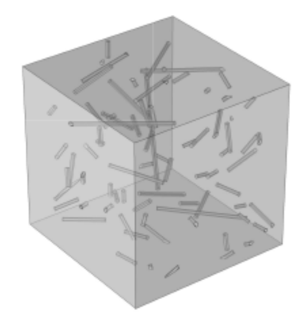

[J. Acoust. Soc. Am. 143, 3283 (2018)]

4.1 Results for fibrous media and discussion

Big picture emerging from these works, enabling to capture **multi-physics** transport phenomena associated with a sound wave propagating through the locally **heterogeneous** fibrous media

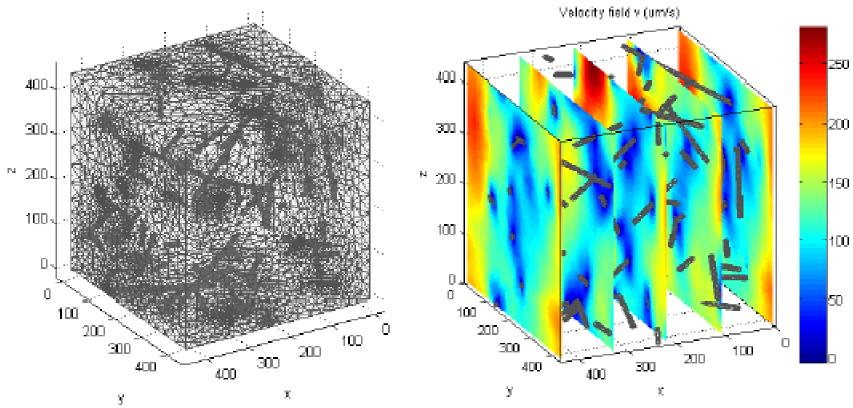

Propagation through the largest interconnected channels

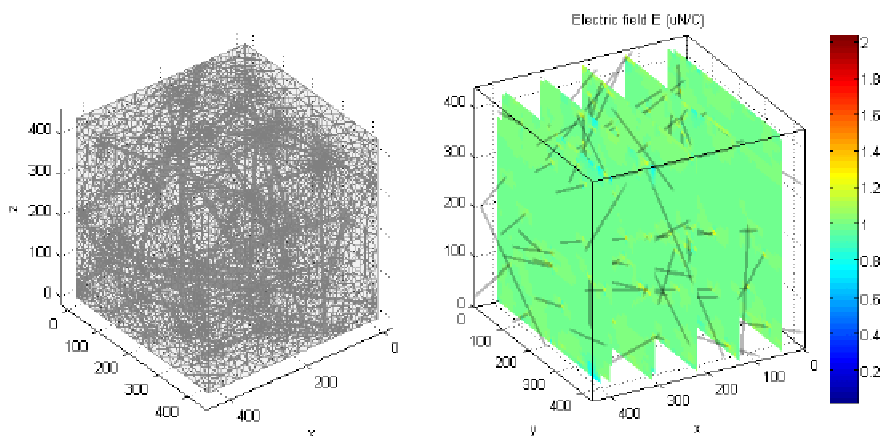

A significant part of the velocity field is carried out by parallel channels of small sizes

Main Results:

- ✓ LF asymptotic behavior, ω→0, the RVE enabling to capture the viscous k_0 and thermal k_0' permeabilities is made from volume weighted fiber diameters.
- ✓ HF asymptotic behavior, ω→∞, the RVE enabling to capture the viscous Λ and thermal Λ' characteristic lengths is made from thin (non-weighted) fiber diameters.

4.2 Results for cellular media and discussion

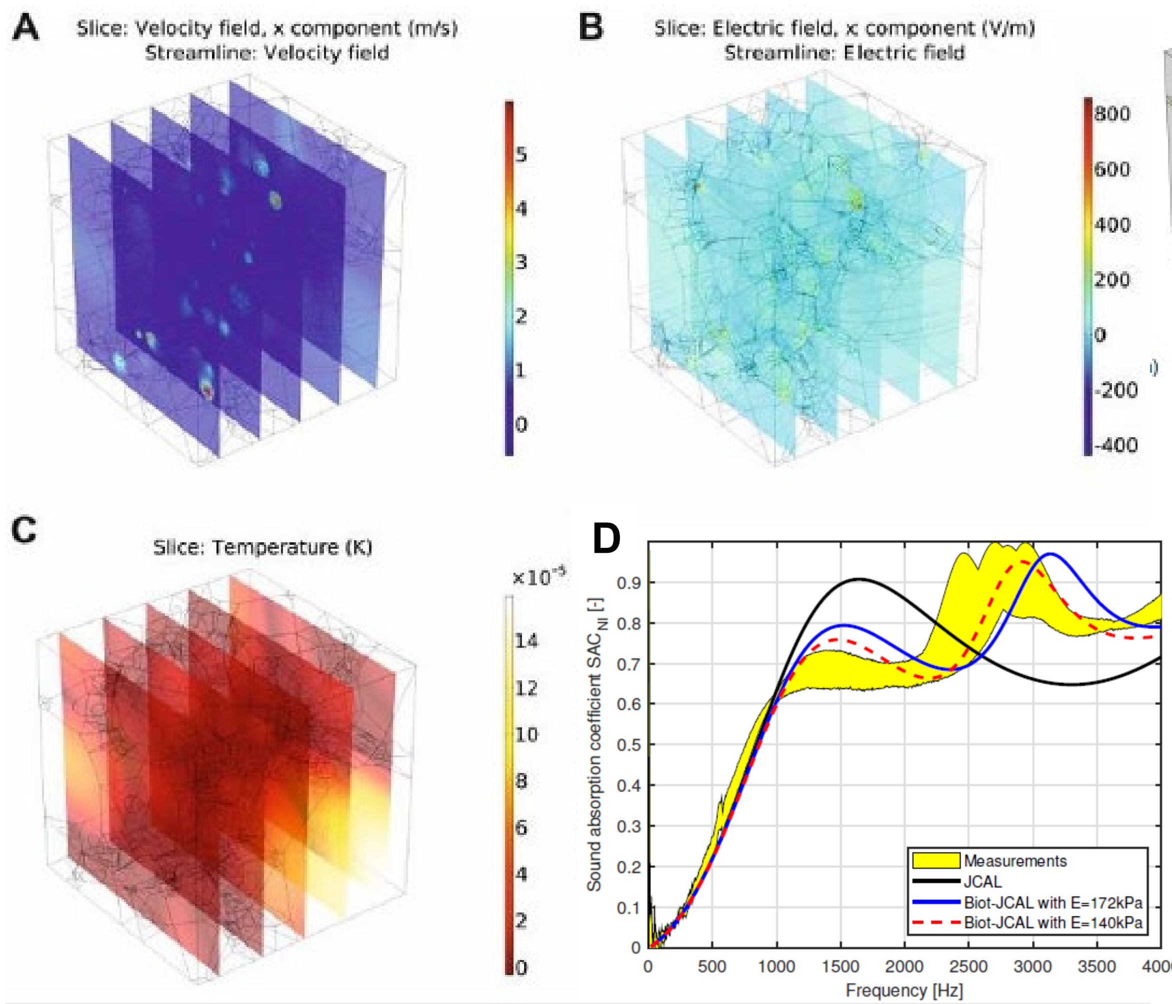

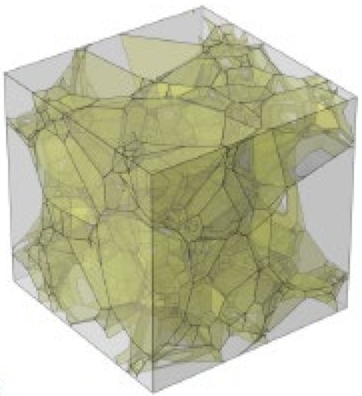

Presence of membranes ↘ k_0 and favors a strong coupling between the fluid and the solid phases

Fig. 4.2.1 Solution fields: (A) Stokes flow. (B) Potential flow. (C) Thermal field. (D) Sound absorption coefficient (SAC_{NI}) computed using JCAL-Biot model with characterized elastic parameters. Sample thickness: 21 mm.

4.2 Results for cellular media and discussion

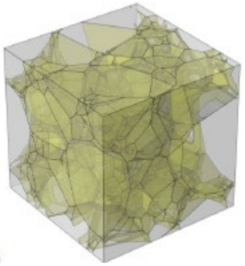

	$\phi\,(-)$	$k_0\,(\times 10^{-10} m^2)$	$\alpha_\infty\,(-)$	$\Lambda\,(\mu m)$	$\Lambda'\,(\mu m)$	$k'_0\,(\times 10^{-10} m^2)$
Measurements	0.92 ± 0.01	2.73 ± 0.34				
Computations		2.83 ± 0.03	3.77 ± 0.35	59 ± 3	270 ± 1	324 ± 8

Tab. 4.2.1 Computed intrinsic transport parameters of a reconstructed random cellular foam without any adjusted parameter, including the characterized distribution of cell size, cell elongation, membranes (proportion and opening ratio)

- A strong anisotropy of the transport properties is induced by the pore size and shape inhomogeneity.
- In average, the computed viscous permeability $2.83 \pm 0.03 \times 10^{-10}\,m^2$ is in good agreement with measured value $2.73 \pm 0.34 \times 10^{-10}\,m^2$.
- Min nb of pores $N_p \geq 50$ to ensure statistical reconstruction of the pore size dist.
- Λ', Λ, k_0' quickly converge ($N_p \sim 4^3$); whereas a REV for k_0 and α_∞ corresponds to $L/\langle d\rangle \sim 10$.

5. Concluding remarks

5.1 Results and discussion

- In this talk, we have provided an overview of the '**stat-of-the-art**' of transport and elastic properties of simulations through acoustic porous materials. In particular, we have concentrated on studies of flow through **three-dimensional** and **random** reconstructed materials (granular, fibrous, cellular foams) at the scale of their **structuring elements** (*grain*, *fiber*, *polyhedron*).
- The most important result is that there is probably not a definitive answer to the questions accompanying the title of this talk. Specifically, we found that the **answer** is rather a **method of analysis** than a typical feature (*observations*, *calculations*, *laboratory measurements*).
- We found however that most of the sound absorbing behavior of a **complex materiel** may generally be related to **two characteristic sizes** (*pore* and *throat size*), an observation which is consistent with the Johnson *et al* semi-phenomenological theory (*asymptotic behaviors*).

5. Concluding remarks

5.2 Where do we stand?

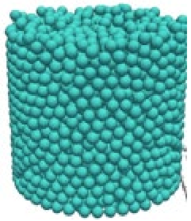

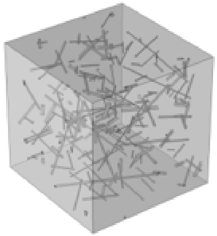

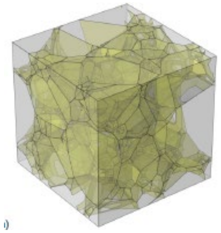

- We have certainly made progress towards the general objective in this talk which was to estimate the intrinsic macroscopic properties of acoustic materials (granular structures, fibrous networks, cellular foams) from easily measurable geometrical properties.
- A general methodology has been implemented in order to calculate the macroscopic properties of these three possible acoustic materials.
- Parametric studies have been performed for generic structures to determine physical trends, and admissible morphological paths to improve material properties.
- What is promising at the moment are

i. multi-functional materials;

ii. controlling disordered effects (polydispersity, local heterogeneity);

iii. coupling effects and hierarchical materials (R. Venegas).

Thank you for your attention !

Acknowledgments

- Invitation: P. Glé, J. Picault, C. Piégay
- Inspiration: P. M. Adler, J. F. Allard, C. Boutin, D. Lafarge
- Historical collaborators : F. Chevillotte, R. Panneton
- Past and present collaborators : K. Attenborough, G. Bonnet, F.-X. Bécot, M. Bornert, M. Cervenka, F. Detrez, L. Gautron, J. Guilleminot, V. Langlois, V. Monchiet, O. Pitois, R. Venegas, T. G. Zielinski
- Industrial collaborators : S. Berger, L. Dejaeger, A. Duval, E. Guillon, M. T. Hoang, G. Jacqus, P. Leroy, V. Marcel
- PhD Students : M. He, M. T. Hoang, A. Kaddami, H. T. Luu, C. T. Nguyen, Q. B. Nguyen, Q. V. Tran, V. H. Trinh